UPDATED RESULTS ON THE LONG-TERM EVOLUTION OF THE SPACE DEBRIS ENVIRONMENT

L. Anselmo, A. Rossi, and C. Pardini

CNUCE Institute, National Research Council (CNR), Via S. Maria 36, 56126 Pisa, Italy

ABSTRACT

The long-term evolution of artificial debris in earth orbit has been analyzed, taking into account a detailed traffic model, explosions, collisions and the effects of air drag. Several scenarios, most of them implementing mitigation measures discussed at international level, have been simulated over a 200-year time span. Moreover, the sensitivity of the results to different collision model assumptions has been assessed.

The simulations confirm the importance of spacecraft and rocket bodies passivation to avoid in-orbit explosions, but the de-orbiting of upper stages is needed as well to curb the debris and collision rate increase and to avert the onset of an exponential growth of artificial objects in the near earth space. The additional removal of end-of-life spacecraft does not improve the outcome dramatically, but may be able to reduce the collision rates in low earth orbit, reversing the historical trend of the last four decades.

Of course, the fragmentation models and the simulation assumptions are still affected by a certain degree of uncertainty, but the results of the sensitivity analysis show that our conclusions are consistent and reliable, at least for the first century.

INTRODUCTION

Artificial orbital debris generated by more than 40 years of space activities are, by now, a common concern for officials and engineers involved in mission design, planning and operations. If left unchecked, they could imperil, in a not too distant future, the exploitation of the near earth space.

Aside from the need to better characterize the present environment down to sub-millimeter sized particles, there is also interest in simulating in a realistic way the long-term evolution of space debris, in order to assess the relative merits and drawbacks of the mitigation measures proposed and discussed at the international level.

In the nineties, a dedicated effort was carried out in Pisa to develop computer codes specifically tailored for the detailed analysis of the long-term evolution of orbital debris (Rossi *et al*., 1998). One of them, the so-called Semi-Deterministic Model (SDM), was designed to follow, as much as possible, the actual orbital evolution of individual space objects. Developed under ESA contract (Anselmo *et al.*, 1996) and upgraded with ASI funding, SDM uses a very fast semi-analytical propagator to compute the orbital evolution of a huge set of objects for very long time spans, under the influence of the atmospheric drag perturbation. Typically, all the largest space objects (corresponding, approximately, to the size class of the catalogued population) and a large sample of the smallest debris (down to 1 mm) may be propagated for one century or more. The sampling factors and the time span allowed depend on the RAM and CPU capabilities of the specific workstation or personal computer used to run the Monte Carlo simulations and may be selected by the user.

SDM includes objects with perigee altitude lower than 40,000 km. Each of them is identified, at any given epoch, by a number, an orbit (semi-major axis, eccentricity, and inclination), and an area-to-mass ratio. The objects

already present in space at the start of a simulation belong to the so-called *historical population*, resulting from past space activities and debris generating events. They are propagated once for all and the results are saved and stored as object density vs. altitude, mass, and time. The *running population* consists, instead, of the objects injected into space after the beginning of a simulation by launches, operations, explosions, and collisions. It is generated and propagated *ex novo* each time a Monte Carlo simulation is run, increased by the source mechanisms (launches and breakups) and decreased by the sink mechanisms (air drag perturbation and active retrievals or de-orbiting). Finally, the *background population*, used to compute the debris collision probability, is obtained at every time step by the sum of the object densities associated both to the historical and running populations.

Complex traffic projections and mitigation scenarios can be modeled in detail, including the possibility of simulating the phased deployment and maintenance of satellite constellations and space stations. In this paper, we present the updated results obtained using new environment and traffic models. The effects, on the low earth orbit environment, of different mitigation measures and model options are illustrated with simulations spanning more than 200 years.

INITIAL DEBRIS ENVIRONMENT

As the initial debris environment, we adopted the 1997.0 CNUCE Orbital Debris Reference Model (Pardini *et al*., 1998). CODRM-97 includes the objects larger than 0.9 mm produced by 140 orbital breakups, 16 liquid metal coolant leaks from nuclear powered spacecraft, international launch activity and space operations.

Each fragmentation or leakage was simulated with the most appropriate models and parameters, and the resulting debris clouds were propagated, including all the significant orbital perturbations, to the chosen reference epoch (January 1, 1997). At this point, the particles still in orbit were merged with the catalogued objects present in space at the same time. In total, more than 65 million particles with mass larger than 1 mg were generated during the simulations and more than 52 million were still in orbit at the reference epoch. The overall cross-sectional area was close to 40,000 m^2, 99.8% of which concentrated in the catalogued population.

Below the altitude of 2000 km, here defined as the low earth orbit (LEO) region, CODRM-97 predicts, on average, 5 million particles larger than 1 mm, 72,000 particles larger than 1 cm and 7200 objects larger than 10 cm. The number of debris crossing this volume of near earth space is, of course, much higher (Pardini *et al.*, 1998).

TRAFFIC MODEL

In order to follow the evolution of the debris population over several decades, it is necessary to define an appropriate traffic model. Due to the rapid change of policy, economic and technological factors, it is practically impossible to foresee the future trends of the international space activities over more than two or three decades. However, we are interested here in a reasonable traffic picture, just to evaluate the relative effectiveness of different debris mitigation solutions discussed at present.

The baseline traffic prediction adopted in this study is quite conservative for the *routine space activity*, for which we assumed a constant launch rate of 79 per year, i.e. that observed in 1997 excluding the Iridium and Orbcom flights. The orbital distribution and the physical characteristics of payloads and upper stages were assumed in agreement with the record of the last five years (1993-1997) and are detailed in Table 1.

Mission related objects of 5 kg, i.e. in the class of the catalogued population, were included as well, reproducing, as far as possible, the observational record. The value adopted (1 per average launch) takes into account the 0.6-0.7 operational debris per launch observed in the last few years plus an additional fraction (0.3-0.4) due to the fact that 1.3-1.4 upper stages are typically left in orbit after each mission. For the Tselina-2 and NOSS/SW-WASS spacecraft, the average number of mission related objects tracked after each launch was used. When more than one upper stage is left in space, the largest one in a long lifetime orbit is taken and represented in the input (as an example, if a Delta 2nd stage and a PAM-D2 motor are both left in a long lifetime orbit, the former is taken).

Space Shuttle and deep space missions are included in the launch statistics, but do not systematically contribute to the terrestrial debris environment, due to the nature of their flights. The *Science* categories in low earth (LEO) and high eccentricity orbit (HEO) are not so precisely defined as the other members of Table 1, because they represent

a very heterogeneous class of *single* missions. So, the overall statistics are correct, but the orbits and the masses of such spacecraft and upper stages are just representative values for a broad range that covers both micro-satellites and large science platforms.

Table 1. Routine Space Activity Model

For each mission profile modeled in our simulations, the table gives the fraction of launches carried out (%), the number of payloads (# of P/L) and mission related objects (# of MRO) associated to each launch, the mass, in kg, and the orbit of payloads (P/L) and upper stages (R/B). The semi-major axis (sma) is given in km, the inclination (inc) in degrees.

Mission	%	# of P/L	P/L mass	P/L sma	P/L ecc	P/L inc	R/B mass	R/B sma	R/B ecc	R/B inc	# of MRO
NASA STS	8.7	1	99999	N/A	N/A	N/A	---	---	---	---	0
GEO Ariane (single)	5.7	1	2000	42164	0.0	0	1240	24478	0.731	6	1
GEO Ariane (double)	6.3	2	1050	42164	0.0	0	1240	24478	0.731	6	1
GEO/GEO Proton	5.0	1	2500	42164	0.0	0	2500	42164	0.01	1	1
GEO/GTO Proton	3.3	1	2500	42164	0.0	0	2500	28575	0.483	15	1
GEO Atlas/Centaur	5.4	1	2000	42164	0.0	0	2300	24478	0.731	25	1
GEO Titan/Centaur	1.7	1	4500	42164	0.0	0	3540	24478	0.731	25	1
GEO Delta II	1.2	1	1050	42164	0.0	0	924	7378	0.071	26	1
GEO CZ-3/CZ-3A	2.4	1	1000	42164	0.0	0	3000	24478	0.731	27	1
GEO H-II	0.2	1	2200	42164	0.0	0	3000	24478	0.731	28	1
Navstar	3.2	1	930	26528	0.0	55	250	15978	0.588	35	1
Glonass	1.7	3	1300	25498	0.0	65	2500	25498	0.0	65	1
Mir servicing	8.7	1	7200	6768	0.0	52	1976	6768	0.0	52	1
Molniya/Oko	4.4	1	1600	26553	0.737	63	900	26553	0.737	63	1
Strela-3/Gonets-D	1.5	6	225	7778	0.0	83	1407	7778	0.0	83	1
Strela-2	0.5	1	875	7168	0.0	74	1443	7168	0.0	74	1
Tselina-D	0.5	1	2000	7028	0.0	83	1407	7028	0.0	83	1
Tselina-2	1.7	1	3250	7228	0.0	71	8300	7228	0.0	71	6
Bion/Foton/Yantar	1.0	1	6500	6653	0.011	63	1976	6653	0.011	63	1
Zenit/Yantar/Kometa	1.2	1	6500	6653	0.011	65	1976	6653	0.011	65	1
Zenit/Yantar/Kometa	2.4	1	6500	6653	0.011	67	1976	6653	0.011	67	1
Zenit/Yantar/Kometa	1.4	1	6500	6653	0.011	65	1976	6653	0.011	65	1
Oblik/Zenit/Resurs	1.5	1	6300	6653	0.011	83	1976	6653	0.011	83	1
7^{th} generation Spysat	0.2	1	10000	6768	0.031	65	8300	6768	0.031	65	1
Parus/Tsikada/Nadez.	3.9	1	825	7368	0.0	83	1443	7368	0.0	83	1
Meteor-2	0.2	1	2000	7328	0.0	83	1407	7328	0.0	83	1
Meteor-3	0.2	1	2215	7578	0.0	83	1407	7578	0.0	83	1
US-P EORSAT	1.9	1	3150	6788	0.0	65	1407	6788	0.0	65	1
Yug/Vector	0.7	1	500	7528	0.113	83	1443	7528	0.113	83	1
New ELINT	0.2	1	5000	8503	0.074	63	4185	8503	0.074	63	1
Okean	0.5	1	1900	7028	0.0	83	1407	7028	0.0	83	1
Geo-IK	0.2	1	900	7828	0.0	74	1407	7828	0.0	74	1
Romb	0.2	1	1000	6868	0.0	66	1443	6868	0.0	66	1
Resurs-O	0.2	1	1900	7038	0.0	98	1407	7038	0.0	98	1
FSW-2	0.7	1	2600	6638	0.014	63	4000	6638	0.014	63	1
Improved Crystal	0.5	1	13500	6878	0.001	98	4500	6878	0.001	98	1
Lacrosse/Vega	0.2	1	14500	7053	0.0	68	4500	6924	0.018	57	1
NOSS/SB-WASS	0.5	3	3000	7528	0.0	63	6500	7528	0.0	63	3
Jumpseat/Trumpet	1.0	1	4500	26428	0.717	63	3540	26428	0.717	63	1
SDS-2	0.2	1	2500	26578	0.745	63	1150	26578	0.745	63	1
Sun-Synchronous	7.8	1	1000	7228	0.0	98	1000	7228	0.0	98	1
HEO Science	4.9	1	1000	26578	0.745	30	1000	26578	0.745	30	1
LEO Science-1	4.0	1	1500	6928	0.0	28	1000	6928	0.0	28	1
LEO Science-2	0.3	1	1000	6978	0.0	70	1000	6978	0.0	70	1
Interplanetary/Lunar	1.9	1	N/A	N/A	N/A	N/A	N/A	N/A	N/A	N/A	N/A

In addition to the routine space activity, reproducing the launch pattern displayed in the past, the injection and maintenance, in low earth orbit, of several commercial satellite constellations was considered as well. From open sources is possible to obtain some general information on the configuration of several constellations at different stages of development. Many parameters, such as the total number of spacecraft and the orbits or the deployment sequence, are still being modified very frequently, reflecting design changes driven by economic and technical reasons. Moreover, some of the systems are uncertain and it is difficult to judge the economic viability of each of them in a market that will be probably characterized by huge capital investments and harsh competition. On the other hand, we are not concerned with business and marketing problems, and our goal is just a realistic analysis (not necessarily precise in every small detail) of the long term interaction of satellite constellations with the orbital debris environment. Therefore, a change of some numbers here and there will not affect the results reported below, as far as the overall picture assumed for our simulations will remain consistent with real world space activities.

Any reference to an existing or proposed constellation is based on the best information available when the simulations were performed. On the other hand, the deployment sequence used was adopted only for simulation purposes; it does not necessarily reflect the plans of the owners/operators or an assessment by the authors. The same applies to the inclusion or not of a particular system in our analysis.

In this study, we assumed the deployment, in between 1997 and 2062, of 20 commercial constellations. Fifteen are similar to projects currently envisaged or under development; five more, modeled on the now defunct M-Star, are wide-band telecommunications systems in LEO (WB-LEO), introduced to cover the far future with a consolidated configuration. A full list of the relevant parameters is given in Tables 2 and 3. The number of satellites in orbit includes spares, if any. The operational life of the constellations takes into account the deployment of new generations of spacecraft in the same satellite system. For the last five constellations, a 200-year life span was considered, just to cover the full simulation length.

Table 2. In-orbit Configuration of the Simulated Satellite Constellations

Constellation Name	Semi-major Axis (km)	Eccentricity	Inclination (deg)	Satellites in Orbit	Spacecraft Mass (kg)
Iridium	7158	0.0	86.4	78	575
Globalstar	7792	0.0	52.0	56	450
Skybridge	7835	0.0	55.0	64	800
Orbcom	7203	0.0	45.0	48	43
Ellipso-Borealis	10561	0.347	116.6	10	174
Ellipso-Concordia	14418	0.0	0.0	12	174
Ico	16733	0.0	45.0	12	2600
Constellation-Ecco	8378	0.0	0.0	12	425
Constellation-Aries	8378	0.0	40.0	35	425
Teledesic	7528	0.0	98.2	324	300
Orblink	15378	0.0	0.0	8	1350
Celestri	7778	0.0	48.0	64	2500
Leo One	7328	0.0	50.0	48	125
Final Analysis	7378	0.0	65.0	44	150
Courier	7178	0.0	76.0	72	100
WB-LEO-1	7728	0.0	47.0	72	1200
WB-LEO-2	7828	0.0	47.0	72	1300
WB-LEO-3	7928	0.0	47.0	72	1400
WB-LEO-4	8028	0.0	47.0	72	1500
WB-LEO-5	8128	0.0	47.0	72	1600

Table 3. Constellations Deployment Schedule Adopted in the Simulations

Constellation Name	Year of First Launch	Spacecraft per Launch	Deployment Launch Rate (yr^{-1})	Maintenance Launch Rate (yr^{-1})	System Lifetime (yr)
Iridium	1997	5	9	1	20
Globalstar	1998	7	4	1	20
Skybridge	2002	4	8	1	20
Orbcom	1997	8	1	1	20
Ellipso-Borealis	2000	5	1	1	20
Ellipso-Concordia	2000	2	2	1	20
Ico	1999	1	4	1	25
Constellation-Ecco	2007	2	3	1	20
Constellation-Aries	2010	5	3	1	20
Teledesic	2001	8	10	1	30
Orblink	2002	2	2	1	20
Celestri	2015	2	10	1	40
Leo One	2010	6	4	1	20
Final Analysis	2015	4	4	1	20
Courier	2020	9	2	1	20
WB-LEO-1	2020	4	6	1	200
WB-LEO-2	2030	4	6	1	200
WB-LEO-3	2040	4	6	1	200
WB-LEO-4	2050	4	6	1	200
WB-LEO-5	2060	4	6	1	200

One upper stage (1500 kg) and two mission related objects (5 kg, each) were associated to every constellation deployment or maintenance launch.

FRAGMENTATION MODELING

In addition to launches, in a typical Monte Carlo run of SDM, the running population is increased by orbital breakups due to explosions and collisions.

Explosions

Explosions are responsible for a large fraction of the current orbiting debris population. Usually they can be classified in two different classes: low and high intensity. In both types, the large-mass end of the mass distribution is well fitted by exponential laws, but for high intensity explosions a power-law tail in the small-mass range must be added, to take into account the generation of a large amount of small fragments. The full details of the simulation models adopted for explosions are discussed elsewhere (Rossi *et al.*, 1998). Based on the historical record of these events, an input file stores, for several classes of spacecraft and upper stages, the typical orbit, mass, explosion rate, fraction of the exploding mass and event category (either low or high intensity explosion). At each time step of a run, a Poisson extractor is used to assess if and which explosions take place, and then these are simulated by the software that generates the corresponding debris.

For this study, we assumed a nominal explosion pattern (exploding objects, explosion rates, exploding mass fraction, breakup orbits) based on the record of the last five years (1993-1997). The relevant parameters are shown in Table 4, including the integral average explosion rate for each event class. The resulting total average explosion rate is 5.2 per year: 2 high intensity explosions, with an effective exploding mass of 120.2 kg, and 3.2 low intensity events, with an effective exploding mass of 2821 kg.

Table 4. Representative Satellite Explosions in Earth Orbit for 1993-1997

Exploding Object	Semi-major Axis (km)	Eccentricity	Inclination (deg)	Mass (kg)	Mass Fraction	Rate (yr^{-1})	Event Class
Proton SOZ (GTO-1)	24300	0.729	47.0	56	1.0	0.6	High
Proton SOZ (GTO-2)	18000	0.629	47.0	56	1.0	0.8	High
Proton SOZ (Glonass)	16130	0.575	65.0	56	1.0	0.4	High
Zenit 2nd stage (LEO)	7230	0.001	71.0	8300	0.1	0.2	Low
Ariane 3rd stage (GTO)	21000	0.682	7.0	1240	1.0	0.6	Low
Russian Spysat (LEO)	6610	0.007	67.0	6200	0.2	0.8	Low
Titan Transtage (GEO)	40000	0.006	12.0	3130	0.3	0.2	Low
H-II 2nd stage (GTO)	24300	0.729	28.5	3000	0.3	0.2	Low
Pegasus HAPS (LEO)	7100	0.015	82.0	97	1.0	0.2	High
Rockot 3rd stage (LEO)	8418	0.019	65.0	1700	0.3	0.2	Low
Russian EORSAT (LEO)	6800	0.005	65.0	3000	0.3	0.2	Low
Titan II 2nd stage (LEO)	6610	0.003	67.0	2860	0.1	0.2	Low
Okean (LEO)	7000	0.005	82.5	1900	0.1	0.4	Low
Proton DM3 (GTO)	24500	0.729	51.4	3400	0.2	0.2	Low

Collisions

For collision events, the fragment mass distribution is based on the assumption that, depending on whether the ratio between the projectile kinetic energy and the target mass is lower or higher than a critical threshold value (the so-called *impact strength* Q^*), we are either in the *cratering regime* (localized damage on part of the target) or in the *catastrophic disruption regime* (complete fragmentation of the target). Reasonable values for the impact strength parameter in the case of artificial orbiting objects lie in the 30,000-60,000 J/kg range (McKnight *et al.*, 1992).

In a catastrophic fragmentation event, the number of objects N having a mass greater than m is assumed to be:

$$N(m) = \left(\frac{m_l}{m} \right)^b , \tag{1}$$

where m_l is the mass of the largest fragment, given by

$$m_l = \frac{1}{2} M_t \left(\frac{M_t Q^*}{E} \right)^{1.24} , \tag{2}$$

E is the kinetic energy of the projectile and M_t is the target mass. The exponent b is given by:

$$b = \left(1 + \frac{m_l}{M_t} \right)^{-1} . \tag{3}$$

In the cratering regime, a similar power-law mass distribution is used, but b is always set equal to 0.8, so that $m_l = M_e /4$, where M_e is the total mass ejected by the impact. $M_e = E /(10Q^*)$, so that the largest possible craters dig 10% of the target mass.

In order to compute the collision rate, the space around the earth is divided in 800 altitude shells, 50 km thick, and the objects in orbit are grouped in 10 logarithmic mass bins, from 10^{-6} to 10^4 kg. The average number of collisions

CN_{jkl} occurring, during the time interval Δt, in the altitude shell h_j, between debris belonging to the couple of mass bins m_k and m_l, can be computed, using the background population density $\rho(m_k,h_j)$, as

$$CN_{jkl} = \pi(r_k + r_l)^2 \frac{\rho(m_k, h_j) v_j \lfloor \rho(m_l, h_j) V_j - \delta_{kl} \rfloor}{1 + \delta_{kl}} \Delta t, \tag{4}$$

where r_k and r_l are the mean projectile and target radii, v_j is the average relative velocity, V_j is the volume of the altitude shell, and δ_{jk} is the Kronecker's symbol. The values obtained, for each pair of mass bins and for every altitude shell, are given in input to a Poisson extractor, which generates positive integer numbers. When the output is not zero, collisions are simulated, assuming for the projectile and target masses the geometric average of their respective mass bin boundaries. The impact velocity is obtained by a random generator, close to the mean pre-computed value given in input, while the target orbit is generated randomly in the appropriate altitude shell. After a collision, both the target and the projectile are removed from the population if the event produces a catastrophic breakup; only the projectile is instead removed if a cratering event takes place. Further details on the collision modeling can be found in Rossi *et al.*(1998).

To compute the effects of collisions, we adopted in this study two different catastrophic disruption thresholds: 40,000 J/kg for 61% of the targets (spacecraft) and 60,000 J/kg for the remaining 39% (rocket bodies). This corresponds to an average value of 47,800 J/kg: however, due to the non-linear nature of the collisional fragmentation law, the influence of the lowest threshold (40,000 J/kg) is stronger in determining the long-term debris evolution.

Area to Mass Ratio

To relate the mass m (kg) and the cross-sectional area A (m^2) of the space objects, included the fragmentation debris, we adopted the classical relationship (Reynolds, 1990):

$$m = \begin{cases} 62.013 A^{1.13} & A \geq 8.04 \cdot 10^{-5} \\ 2030.33 A^{1.5} & A < 8.04 \cdot 10^{-5} \end{cases} . \tag{5}$$

Object diameters were obtained assuming a spherical shape. For explosions and collisions, the mass of each fragment was used to compute a corresponding average cross-section by inverting Eq. 5; then, the actual area was randomly extracted from an appropriate log-normal distribution (Anselmo *et al.*, 1996).

For the catalogued objects, when the mass was known with a reasonable level of confidence, the corresponding area was obtained using Eq. 5. On the other hand, if reasonable values for the mass were not available, the measured radar cross section (RCS) was equated to the area and the corresponding mass was finally computed, again with Eq. 5. The Mie and Rayleigh radar scattering regimes were not taken into account, but for 1 m^2 > RCS > 0.01 m^2 the corrections involved were comparable to the uncertainties associated with the debris shape and radar reflectivity (Badhwar and Anz-Meador, 1989). Moreover, there were only a few objects with RCS < 0.01 m^2 and the effect on the computation of the collision probabilities between mass bins was negligible.

MITIGATION SCENARIOS

In order to evaluate the effectiveness of several debris mitigation measures discussed at present, we simulated several scenarios for a 200-year time span. Of course, most of the basic assumptions might fail in such a long time interval, but only by looking at the results of very long simulations it is possible to evaluate the measures to be taken in the next few decades, outside the confounding fog of a few stochastic events. In other words, to clearly understand what is best to do in the near future, we must propagate the effects of any action taken for one century or more. Therefore, a long time span is used not to provide accurate, and meaningless, debris predictions after one or two centuries, but to put in a clearer perspective the situation in orbit in the next two or three decades.

The results for each scenario were obtained averaging 10 different Monte Carlo simulations carried out with SDM, in order to smooth out the stochastic effects and exhibit the main trends of the evolution. The full near earth space, up to the height of 40,000 km, was included in the computations, but in this paper, for lack of space, we can present only the outputs for the low altitude region, below 2000 km. The scenarios considered are:

1. Business as usual (BAU): includes a constant routine launch rate of 79 per year (as given in Table 1) plus the commercial satellite constellations (Table 2), following the deployment and maintenance schedule given in Table 3. No mitigation measure is adopted: all the upper stages are left in orbit according to their mission profile and the in-orbit explosions follow the pattern given in Table 4. In particular, constellation upper stages and satellites no longer operational are left in orbit, but we assume that the operational spacecraft of a given constellation cannot collide between them, as they are supposed to be controlled;
2. No explosion (NOEX): as BAU, but with both spacecraft and rocket bodies effectively passivated at the end of their life, to completely prevent in-orbit explosions after 2010. Because the explosions involving objects that had been in orbit more than 5 and 10 years were less than 5% and 1.4%, respectively, the scenario simulated is very close to the generalized introduction of passivation measures a few years before 2010;
3. De-orbiting of upper stages (DEOUP): as NOEX, but with the de-orbiting of all the new rocket bodies, with perigee altitude below 2000 km, launched after 2010. Constellation upper stages are de-orbited as well, below 2000 km, according to their deployment and maintenance launch schedule;
4. De-orbiting of constellation spacecraft (DEORCO): in addition to the mitigation measures considered in the DEOUP scenario, all the constellation satellites below 2000 km are de-orbited at the end of life, when replaced by another spacecraft according to the maintenance launch schedule. Therefore, only operational spacecraft (in-orbit spares included) are assumed to be in space, at any given time, in low earth orbit. When a constellation in the same orbital regime completes its mission, all the spacecraft of the system are removed from space;
5. De-orbiting of all the spacecraft (DEOALL): in addition to the DEORCO mitigation actions, all the spacecraft (not belonging to commercial constellations) in high eccentricity orbits, with perigee altitude below 2000 km, or in near circular orbits, in between 600 and 2000 km, are de-orbited at the end of life, after 2030.

SIMULATION RESULTS

Figures 1, 2 and 3 show the long-term evolution, below 2000 km, of the number of debris larger than 0.1, 1 and 10 cm, respectively. The collision rate evolution, for the same size classes, is shown in Figures 4, 5 and 6.

The elimination of in-orbit explosions seems to be the single most effective measure to limit the growth of decimeter sized debris, which are the projectiles able to breakup a satellite. However, the collision rate in that size class is only slightly reduced, due to the increasing number of spacecraft and upper stages, that account for most of the collisional cross-section. A significant improvement is obtained only through the de-orbiting of the new rocket bodies launched in space, while the further removal of spacecraft at the end of life is useful (the number of objects and the collision rate decrease), but the proportional gain is smaller.

Most of the same conclusions apply to centimeter sized debris, produced in large numbers both by explosions and collisions (craterizations included). For millimeter sized particles the overall picture is similar, but explosions are a less important source and the relative contribution of upper stages de-orbiting is even more important. On the other hand, only the adoption of all the mitigation measures analyzed here (DEOALL scenario) can guarantee a long-term reduction of the collision rates and a very slow growth of the debris population in low earth orbit.

Sensitivity Analysis

The long-term debris evolution is mainly driven by collisions. To assess how the predictions are affected by the collisional model assumptions, the baseline BAU scenario was also run with different impact strength values (30,000 and 60,000 J/kg, each uniformly applied to all the population), or adopting the NASA's EVOLVE fragmentation model (Reynolds, 1991). Ten standard Monte Carlo runs were carried out in each case, and the averaged results are presented here.

Figures 7, 8 and 9 show the debris population evolution as a function of the target impact strength. The simulated values probably include the full range of reasonable fragmentation thresholds for spacecraft and upper stages. After 100 years the differences are still moderate, and even after 200 years the worst case (Q^* = 30,000 J/kg) produces a

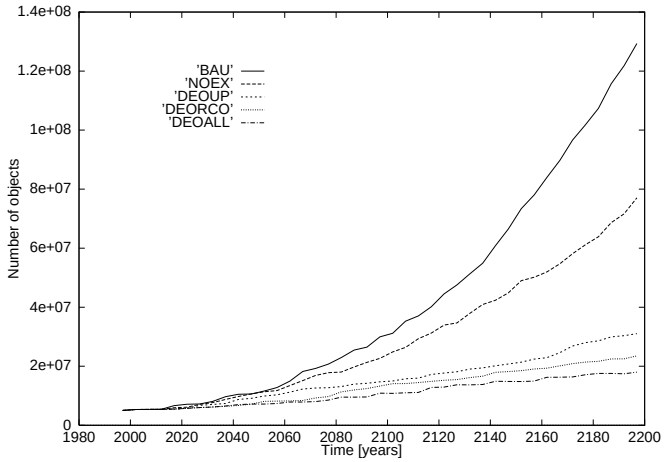

Fig. 1. Number of orbital debris larger than 1 mm (below 2000 km) for the five simulated scenarios.

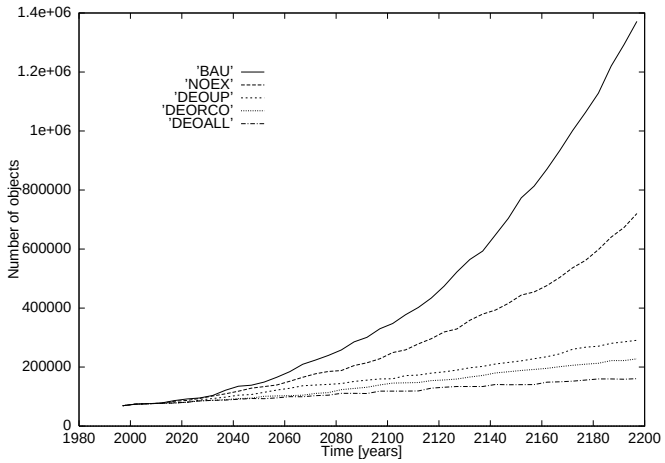

Fig. 2. Number of orbital debris larger than 1 cm (below 2000 km) for the five simulated scenarios.

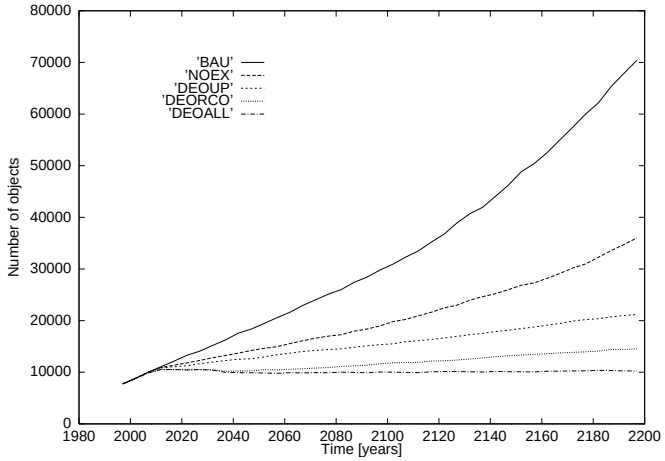

Fig. 3. Number of orbital debris larger than 10 cm (below 2000 km) for the five simulated scenarios.

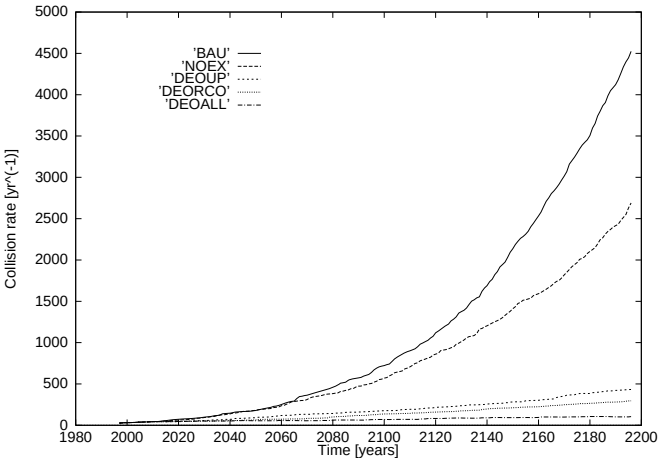

Fig. 4. Collision rate for orbital debris larger than 1 mm (below 2000 km) for the five simulated scenarios.

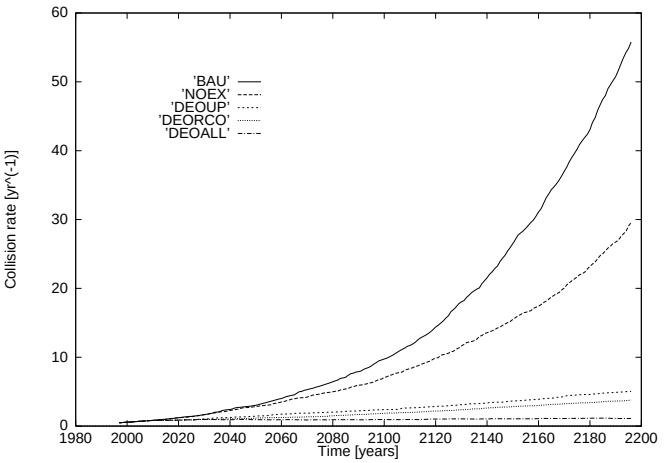

Fig. 5. Collision rate for orbital debris larger than 1 cm (below 2000 km) for the five simulated scenarios.

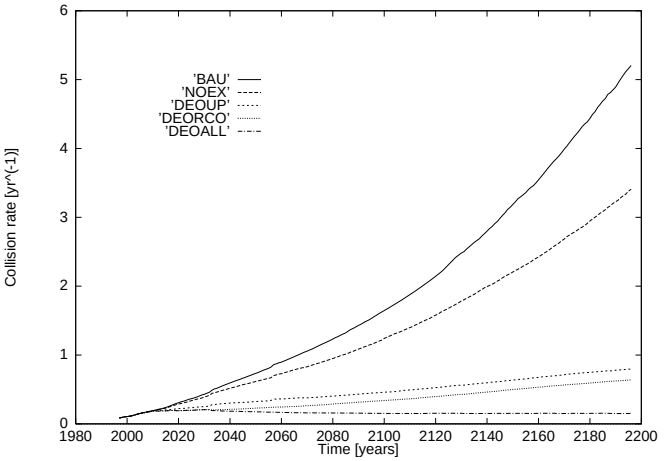

Fig. 6. Collision rate for orbital debris larger than 10 cm (below 2000 km) for the five simulated scenarios.

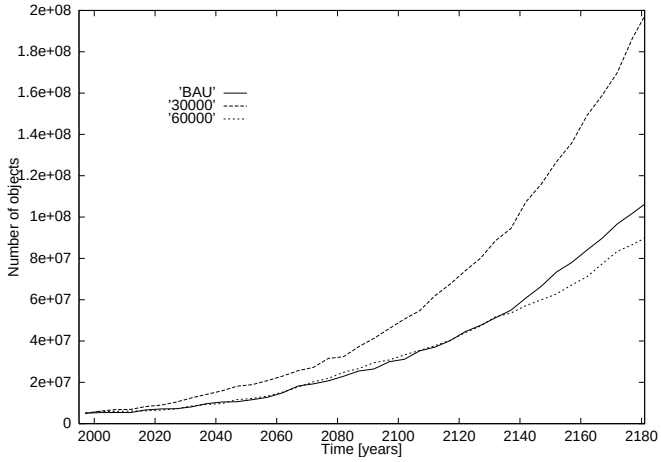

Fig. 7. Number of orbital debris larger than 1 mm (below 2000 km) for 30,000 J/kg ≤ Q^* ≤ 60,000 J/kg.

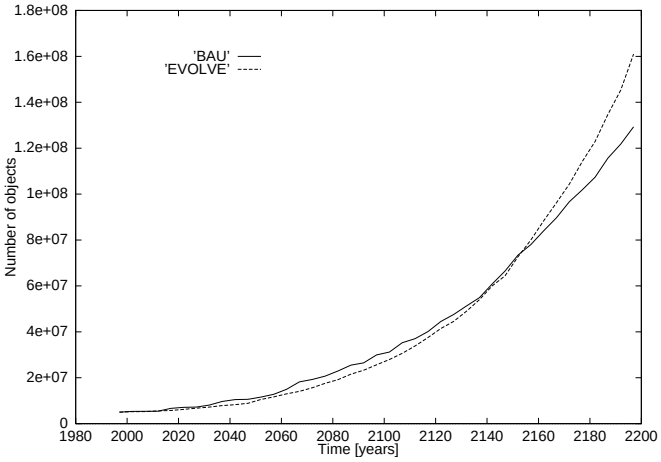

Fig. 10. Comparison between fragmentation models for collisions (debris larger than 1 mm below 2000 km).

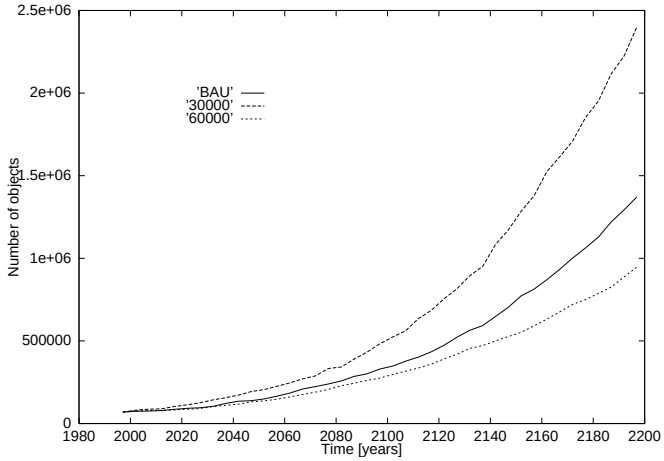

Fig. 8. Number of orbital debris larger than 1 cm (below 2000 km) for 30,000 J/kg ≤ Q^* ≤ 60,000 J/kg.

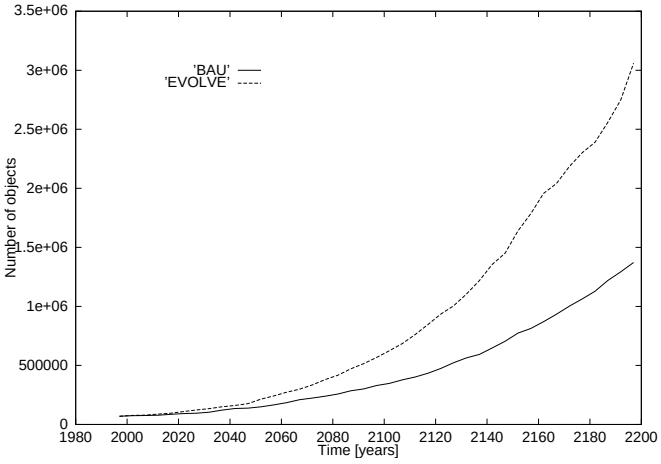

Fig. 11. Comparison between fragmentation models for collisions (debris larger than 1 cm below 2000 km).

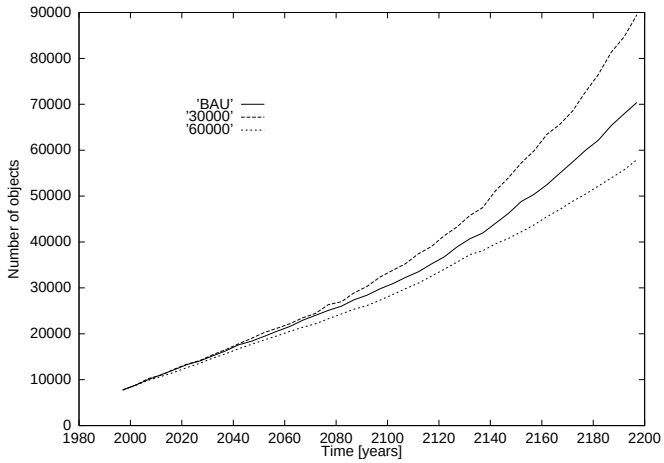

Fig. 9. Number of orbital debris larger than 10 cm (below 2000 km) for 30,000 J/kg ≤ Q^* ≤ 60,000 J/kg.

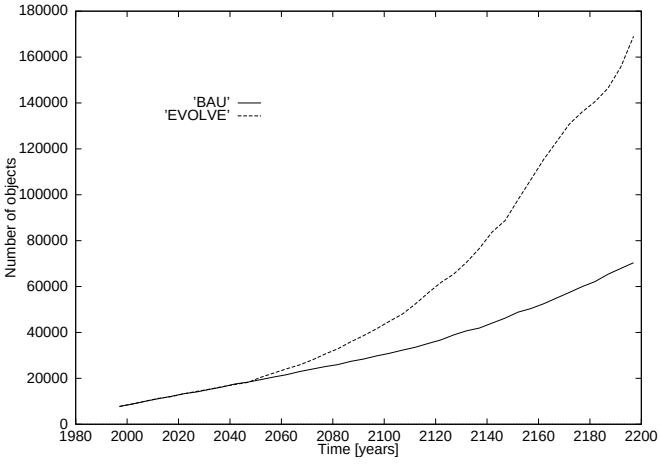

Fig. 12. Comparison between fragmentation models for collisions (debris larger than 10 cm below 2000 km).

number of millimeter sized particles just a factor 2 larger than the baseline BAU scenario. The differences for bigger debris are smaller.

Figures 10, 11 and 12 show the comparison with the EVOLVE fragmentation model for collisions. The simulation with the EVOLVE model generates a larger number of debris of any size, but the results are very close for millimeter sized particles, while the agreement goes progressively worse with the increase of the objects size (after 200 years, the number of decimeter sized objects is 2.4 times that given by the baseline BAU scenario). However, after one century the differences are still quite limited.

CONCLUSIONS

Very long-term simulations of the orbital debris environment are needed to evaluate the relative effectiveness of different mitigation measures. The results of our updated analysis confirm the importance of spacecraft and rocket bodies passivation to avoid in-orbit explosions (Rossi *et al*., 1997), but the de-orbiting of upper stages is needed as well to curb the debris and collision rate increase and to avert the onset of an exponential growth for a couple of centuries, or more. The additional removal of end-of-life spacecraft does not improve the outcome dramatically, but may be able to reduce the collision rates in low earth orbit for any size range above 1 mm, reversing the historical trend of the last four decades.

Of course, the fragmentation models and the simulation assumptions are still affected by a certain degree of uncertainty, but the results of the sensitivity analysis show that our conclusions are qualitatively, and quantitatively (at least for the first century) consistent and reliable.

ACKNOWLEDGMENTS

The work described in this paper has been carried out in the framework of the Cooperation Agreement (1997-2001) between the CNUCE Institute of the National Research Council (CNR) and the Italian Space Agency (ASI).

REFERENCES

Anselmo, L., A. Cordelli, P. Farinella, C. Pardini, and A. Rossi, *Study on Long Term Evolution of Earth Orbiting Debris - Final Report*, ESA/ESOC Contract No. 10034/92/D/IM(SC), Consorzio Pisa Ricerche (1996).

Badhwar, G.D., and P.H. Anz-Meador, Determination of the Area and Mass Distribution of Orbital Debris Fragments, *Earth, Moon and Planets*, **45**, 29 (1989).

McKnight, D.S., R.L. Maher, and L. Nagl, *Fragmentation Algorithms for Satellite Targets (FAST) Empirical Breakup Model, Version 2*, Kaman Sciences Corporation (1992).

Pardini, C., L. Anselmo, A. Rossi, A. Cordelli, and P. Farinella, The 1997.0 CNUCE Orbital Debris Reference Model, in *Spaceflight Mechanics 1998*, paper AAS 98-173, Advances in the Astronautical Sciences Series, **99**, Univelt Inc., San Diego, CA (1998).

Reynolds, R.C., Review of Current Activities to Model and Measure the Orbital Debris Environment in Low-Earth-Orbit, *Advances in Space Research*, **10**, No. 3-4, 359 (1990).

Reynolds, R.C., *Documentation of Program EVOLVE: A Numerical Model to Compute Projections of the Man-made Orbital Debris Environment*, SPC Report No. OD91-002-U-CSP, System Planning Corporation (1991).

Rossi, A., L. Anselmo, C. Pardini, P. Farinella, and A. Cordelli, Interaction of the Satellite Constellations with the Low Earth Orbit Debris Environment, *International Workshop on Mission Design & Implementation of Satellite Constellations*, Toulouse, France, 17-19 November (1997).

Rossi, A., L. Anselmo, A. Cordelli, P. Farinella, and C. Pardini, Modelling the Evolution of the Space Debris Population, *Planetary and Space Science*, **46**, No. 8, in press (1998).